Detailed $^{40}Ar/^{39}Ar$ dating of geologic events associated with the Mantos Blancos copper deposit, northern Chile

Verónica Oliveros · Gilbert Féraud · Luis Aguirre · Luis Ramírez · Michel Fornari · Carlos Palacios · Miguel Parada

Abstract The $^{40}Ar/^{39}Ar$ geochronological method was applied to date magmatic and hydrothermal alteration events in the Mantos Blancos mining district in the Coastal Cordillera of northern Chile, allowing the distinction of two separate mineralization events. The Late Jurassic Mantos Blancos orebody, hosted in Jurassic volcanic rocks, is a magmatic-hydrothermal breccia-style Cu deposit. Two superimposed mineralization events have been recently proposed. The first event is accompanied by a phyllic hydrothermal alteration affecting a rhyolitic dome. The second mineralization event is related to the intrusion of bimodal stocks and sills inside the deposit. Because of the superposition of several magmatic and hydrothermal events, the obtained $^{40}Ar/^{39}Ar$ age data are complex; however, with a careful interpretation of the age spectra, it is possible to detect complex histories of successive emplacement, alteration, mineralization, and thermal resetting. The extrusion of Jurassic basic to intermediate volcanic rocks of the La Negra Formation is dated at 156.3±1.4 Ma (2σ) using plagioclase from an andesitic lava flow. The first mineralization event and associated phyllic alteration affecting the rhyolitic dome occurred around 155–156 Ma. A younger bimodal intrusive event, supposed to be equivalent to the bimodal stock and sill system inside the deposit, is probably responsible for the second mineralization event dated at ca. 142 Ma. Other low-temperature alteration events have been dated on sericitized plagioclase at ca. 145–146, 125, and 101 Ma. This is the first time that two distinct mineralization events have been documented from radiometric data for a copper deposit in the metallogenic belt of the Coastal Cordillera of northern Chile.

Keywords $^{40}Ar/^{39}Ar$ · Cu mineralization · Jurassic · Coastal Cordillera · Chile

V. Oliveros (✉) · L. Aguirre · L. Ramírez · C. Palacios · M. Parada
Departamento de Geología, Universidad de Chile,
P.O. Box 13518-21, Santiago, Chile
e-mail: volivero@ing.uchile.cl

G. Féraud · M. Fornari
CNRS-IRD-UNSA UMR 6526 Géosciences Azur,
Université de Nice-Sophia Antipolis—Parc Valrose,
06108 Nice, France

V. Oliveros
Departamento de Ciencias de la Tierra,
Universidad de Concepción,
P.O. Box 160-C, Concepción, Chile

Introduction

The Coastal Cordillera of northern Chile hosts numerous copper deposits, constituting a NS-trending Late Jurassic to Early Cretaceous metallogenic belt extending 200 km from 22° to 24°S (Fig. 1). This metallogenic belt represents an important source of Chilean copper production (Maksaev and Zentilli 2002). Total annual production of fine copper from these deposits is on the order of 230,000 ton, primarily from the exploitation of six orebodies. The major mines currently operating are located in the Mantos Blancos mining district, which produces 50% of the copper from the belt and has estimated resources of 500 million ton with 1.0% Cu. Two types of ore deposits occur in this copper belt: volcanic-hosted stratabound orebodies (Espinoza et al. 1996; Maksaev and Zentilli 2002) and porphyry

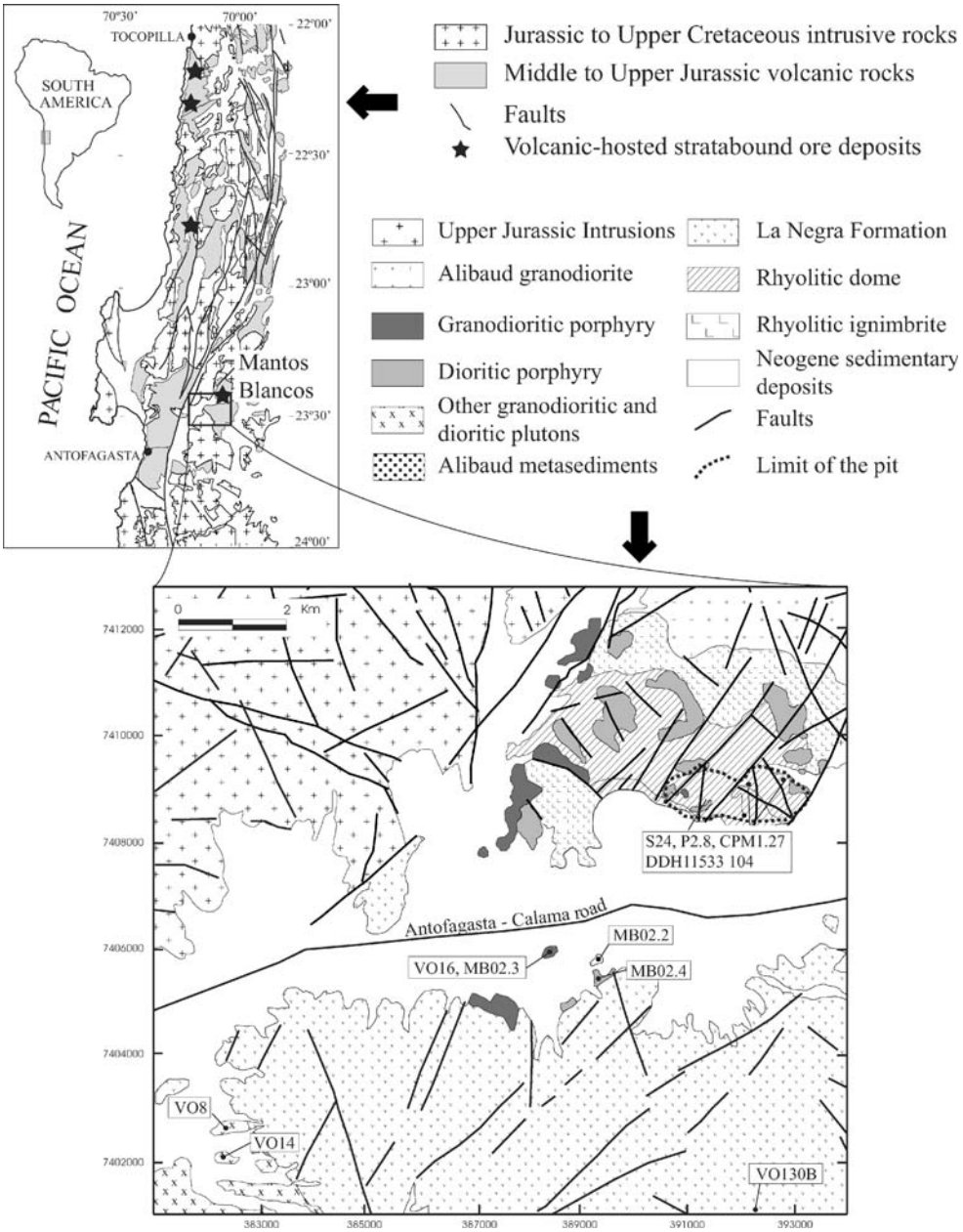

Fig. 1 Simplified geology map of the Coastal Cordillera between 22°00′ and 24°00′S. Other volcano-hosted, strata-bound type copper deposits are also shown. *Inset*: geology of the Mantos Blancos district, modified after Ramírez et al. (2006)

copper deposits (Camus 2003). The stratabound orebodies have long been known as "Chilean manto-type," because initial mining exploited the stratiform section of these deposits. However, they are characterized by central hydrothermal breccias that form feeder structures to the flat-lying stratiform peripheral mineralization. The magmatic-hydrothermal breccias host half of the mineralization and have the highest ore grade in the deposits. These breccias are genetically related to coeval dioritic to granodioritic stocks and sills and are intruded by post-mineralization dioritic dikes and stocks. Hypogene sulfide mineralization consists of bornite, digenite, and chalcopyrite related to sodic hydrothermal alteration (Palacios 1990; Ramírez et al. 2006).

In spite of their importance, the ages of the copper ore deposits of the Coastal Cordillera in northern Chile are not well known. This applies to the volcanic rocks that host the main ore deposits, the intrusive bodies related to mineralization, and the associated hydrothermal processes. Only scarce K/Ar and Rb–Sr ages between 160 and 130 Ma (Michilla, Buena Esperanza, and Mantos Blancos) have been published (e.g. Chávez 1985; Boric et al. 1990; Tassinari et al. 1993; see discussion by Maksaev and Zentilli 2002). Recently, a Re–Os age of 159±16 Ma (2σ) on chalcocite from the main deposit in the Michilla mining district (22°30′S) has been reported (Tristá-Aguilera et al. 2006); an interval of 163.5±1.9 and 157.4±3.6 Ma has also been proposed for

the main mineralization event in this deposit (Oliveros et al. 2007).

The present paper reports a detailed $^{40}Ar/^{39}Ar$ study on most of the geological formations of the Mantos Blancos district, including intrusive and volcanic rocks and secondary minerals, allowing to determine a chronological evolution of the ore deposits in the district. The ore deposits cannot be easily and precisely dated directly, and this paper shows how a careful interpretation of complex geochronological data obtained on igneous and secondary products can indirectly give precise ages for the ore deposits. This geochronological model is largely based on field observations that are given by Ramírez et al. (2006), who recently proposed a comprehensive two-stage evolution model of the hydrothermal system of the Mantos Blancos ore deposit. In particular, our geochronological data are in agreement with the two mineralization events hypothesized by Ramírez et al. (2006).

Geologic and tectonic setting

Since the Early Jurassic, subduction-related magmatism developed along the Coastal Cordillera. The Jurassic volcanic activity is represented by the La Negra Formation, a 7,000-m thick sequence of mainly basaltic to andesitic lavas with calc–alkaline and minor tholeiitic affinities and sedimentary rocks (García 1967; Palacios 1978, 1984; Rogers and Hawkesworth 1989; Pichowiak 1994; Kramer et al. 2004). Based on radiometric ages and paleontological evidence obtained on marine sedimentary intercalations, the extrusive event has been bracketed between Early Jurassic and Oxfordian (Rogers and Hawkesworth 1989; Basso 2004; Kramer et al. 2004; Oliveros et al. 2006; Cortés et al. 2007), with an apparent maximum of volcanic activity during the Late Jurassic (Callovian to Kimmeridgian age, Oliveros et al. 2006). The volcanic sequence was intruded by Early Jurassic (ca. 173–190 Ma) and Late Jurassic (ca. 142–160 Ma) tonalitic-granodioritic and dioritic plutonic rocks (Pichowiak et al. 1990; Andriessen and Reutter 1994; Pichowiak 1994; Dallmeyer et al. 1996; Scheuber 1994; Scheuber and González 1999; Oliveros et al. 2006). Similar isotopic compositions of both the volcanic and plutonic rocks suggest mantle-derived parental magmas with minor or no crustal contamination (Rogers and Hawkesworth 1989; Lucassen and Franz 1994; Kramer et al. 2004).

The Coastal Cordillera tectonic evolution during the Jurassic is interpreted in terms of a transtensional regime because of oblique subduction (Scheuber and González 1999) and/or to a retreating type boundary system (Grocott et al. 1994). A major arc-linked structure, the Atacama Fault System (AFS), concentrated most of the deformation in the arc during the Jurassic and Early Cretaceous with sinistral strike–slip motion. During the Paleogene Incaic compressive phase, the AFS was reactivated, and the present day Coastal Cordillera of northern Chile was probably formed at this time (Arraigada 2003).

Geology of the Mantos Blancos mining district

The Mantos Blancos ore deposit is hosted within a rhyolitic dome that is supposed to be associated with hydrothermal breccias, which in turn are intruded by bimodal stocks and sills of dioritic and granodioritic composition (Fig. 1), causing a second stage of brecciation and hydrothermal alteration (Ramírez et al. 2006). All these lithological units are mineralized to different degrees (Ramírez et al. 2006). A late mineralization dioritic dyke swarm crosscuts all the exposed rock units. The eastern and western boundaries of the Mantos Blancos ore deposit are marked by NNE to NS-trending faults, which separate the ore deposit from Lower Jurassic tonalitic plutonic rocks (Fig. 1). To the north, the igneous rocks that host the ore deposit intrude a Lower to Middle Jurassic granodiorite (Cortés et al. 2007; Fig. 1). To the south, the ore deposit is limited by an ENE-trending fault, separating it from the Jurassic andesitic to basaltic sequence of the La Negra Formation (Cortés et al. 2007). In much of the district, the fault is covered by Quaternary sediments (Fig. 1); therefore, the stratigraphic relationship between the host rhyolitic dome and the La Negra sequence is unclear.

Dioritic and granodioritic porphyries also crop out 5 km to the S and SW of the main ore deposit (Fig. 1) and appear to be equivalent to the Mantos Blancos bimodal porphyry based on similarities in texture and mineralogical and geochemical composition. Additionally, other small bodies of equigranular granodiorite to diorite also crop out 8 km southwest of the deposit (Fig. 1); however, there is no evidence of a correlation between these rocks and the bimodal porphyry stocks and sills.

The geology of the Mantos Blancos ore deposit is described in detail by Ramírez et al. (2006), who recognized two superimposed hydrothermal events. The first event is coeval with the magmatic-hydrothermal brecciation and its associated phyllic alteration. The hypogene assemblage of this first event consists of chalcopyrite, pyrite, bornite, quartz, and sericite. This assemblage occurs in various modes, including: (a) isolated crystals within quartz phenocrysts of the breccias, (b) disseminated crystals in the felsic dome and in the matrix and fragments of the hydrothermal breccia, and (c) in veinlets. The assemblage is observed in deep drill cores within the rhyolitic dome, at least 300 m away from breccia pipes of the second hydrothermal event (Ramírez et al.

2006). The second event represents the main stage of hydrothermal activity, during which three types of hydrothermal alteration occurred: potassic (K–feldspar, quartz, tourmaline, biotite, chlorite, and magnetite), propylitic (quartz, chlorite, epidote, calcite, albite, hematite, and galena), and sodic (albite, hematite). Mineralization associated with this event consists of chalcopyrite, pyrite, and digenite. These minerals occur as disseminated crystals or as stockworks in the felsic dome, bimodal porphyries, and in the matrix of the dioritic to granodioritic magmatic-hydrothermal breccias. Mineralization in veinlets crosscutting phyllic veins of the first event also occur. Finally, late-ore mafic dikes intruded all of the rock units within the Mantos Blancos copper deposit (Ramírez et al. 2006).

On a regional scale, a widespread low-grade alteration with a typical propylitic assemblage of quartz, chlorite, epidote, calcite, sericite, and titanite affects the volcanic rocks of the La Negra Formation. This alteration is thought to be equivalent to the "alteration on regional scale," defined by Losert (1974).

Description of the analyzed samples

Three samples of granodioritic and dioritic porphyries located 3 km S and SW from the Mantos Blancos ore deposit, VO16, MB02.4, and MB02.3, as well as one sample (VO8) of an equigranular granodiorite intrusion located 8 km to the SW, were analyzed (Fig. 1). These rocks contain plagioclase, potassic feldspar, quartz, biotite, and hornblende. With the exception of sample VO8, biotites from the intrusive rocks are commonly chloritized, while hornblende crystals remain fresh. Sample VO14 was collected near VO8 (Fig. 1) and belonged to a strongly altered intrusion, probably a granodiorite, with quartz, sericitized plagioclase, and altered mafic minerals. As mentioned previously, whereas VO16, MB02.4, and MB02.3 are thought to be related to the bimodal stocks and dykes inside the Mantos Blancos ore deposit because of their similar petrological and geochemical features, the pluton corresponding to the sample VO8 has no direct correlation with any units known in the deposit.

Sample MB02.2 is an andesite from the La Negra Formation affected by contact metamorphism, probably related to the emplacement of the dioritic and granodioritic porphyries located nearby and described above (Fig. 1). The sample has an hornfelsic texture with plagioclase, biotite, and amphibole in the groundmass and replacing primary plagioclase and pyroxene phenocrysts. Sample VO130B is a basaltic-andesitic lava flow from the La Negra Formation sampled about 7 km south of the Mantos Blancos deposit. The rock is rich in plagioclase phenocrysts, which are strongly sericitized but contain fresher cores; chlorite and epidote are also present as alteration phases in the groundmass and mafic phenocrysts.

Sample CPM1.27 is from a late-mineralization monzonitic dyke, which crosscuts the magmatic-hydrothermal breccias, feeders of the second mineralization event. It contains traces of pyrite and chalcopyrite together with a weak propylitic and albitic alteration; therefore, its age should represent a late stage of the second mineralization event. Plagioclase, potassic feldspar, and amphibole phenocrysts in this rock are strongly altered. Despite this strong alteration, the abundant amphibole phenocrysts (up to 50% of the rock) preserve large fresh internal zones.

Sample S.24 is a dioritic rock collected from drill core, whereas sample P2.8 is a dioritic dyke. In the case of sample S24, the contact relationship with the host rocks is not clear. Both samples might belong to the basic dyke swarm that crosscuts the rhyolitic dome, as their basic chemical composition is very similar and strongly contrasts to that of the acid host rocks. These plagioclase-rich porphyritic rocks contain mafic minerals that are mostly chloritized and small amounts of pyrite and traces of chalcopyrite.

Sample DDH11533-104 is a sample of a drill core from the rhyolitic dome that is weakly mineralized. The sample was taken under the main orebody and contains quartz, plagioclase, biotite, and other mafic minerals as phenocrysts and within the felsitic groundmass. The plagioclase phenocrysts are intensely seritized and albitized, biotites are replaced by iron-rich minerals and other mafic phenocrysts are completely chloritized.

Analytical procedures

Fifteen primary and secondary minerals from 11 rock samples were analyzed using the $^{40}Ar/^{39}Ar$ step-heating method. Analyzed primary minerals include: single grains of biotite from samples VO8 and VO16, bulk plagioclase from samples VO130B, S24, and P2.8, small clusters of amphibole grains from samples MB02-3, MB02-3, and MB02.4 (heated with a laser system), and a bulk sample of amphibole from sample VO16, which was heated with a high frequency furnace (HF). Analyzed secondary minerals consisted of strongly sericitized plagioclase single grains from samples VO14, VO130B, DDH11533, S24, and P2.8, all of which were heated with a laser system. Mineral separation was carried out using a Frantz magnetic separator followed by careful hand picking under a binocular microscope. Grain sizes are 300–500 μm for sericitized plagioclase and biotite single grains and 125–200 μm for amphibole and fresh plagioclase populations. The weight of the analyzed samples was 0.05–0.8 mg for biotite and sericitized plagioclase single grains, 1.2–1.5 mg

for amphibole and plagioclase bulk sample heated with the laser system, and 8.7 mg for the amphibole bulk sample (VO16) heated with the HF furnace. The samples were packed into copper or aluminum foils for the HF furnace or laser experiments, respectively. The samples were then irradiated for 70 h in the Hamilton McMaster University nuclear reactor (Canada) in position 5C along with the Hb3gr hornblende monitor for which an age of 1,072 Ma is adopted (Turner et al. 1971; Renne et al. 1998; Jourdan et al. 2006). The total neutron flux density during irradiation was about 8.8×10^{18} n/cm^2. The estimated error bar on the corresponding ^{40}Ar*/^{39}ArK ratio is ±0.4% (2σ) in the volume where the samples were included. For the samples heated with the laser system (Synrad 48–5 CO_2 laser), isotopic measurements were performed with a VG3600 mass spectrometer equipped with a Daly system and a photomultiplier. For the samples heated with the HF furnace, the analysis was performed with a mass spectrometer composed of a 120° M.A.S.S.E. tube, a Baür–Signer GS 98 source and a SEV217 Balzers electron multiplier. Total blanks were measured every third step on the laser system and every third sample on the HF furnace system. Argon isotopes were typically on the order of 20–2,000, 100–15,000, and 1–50, for laser experiments, and on the order of 30–430, 10–7,000, and 8–50, for HF furnace experiments, times the blank level for ^{40}Ar, ^{39}Ar and ^{36}Ar, respectively.

The criterion used to define a plateau age includes: (1) at least 70% of the ^{39}Ar released; (2) a minimum of three successive steps in the plateau; and (3) the integrated age of the plateau should agree with each apparent age of the plateau within a two sigma (2σ) confidence level. Plateau and integrated ages are given at the 2σ confidence level. The uncertainties on the ^{40}Ar/^{39}Ar ratios of the monitors are included in the calculation of the integrated and plateau age uncertainties, but the error on the age of the monitor is not included.

The chemical compositions of the primary and secondary minerals were obtained using a CAMECA SX-100 electron microprobe at the Institut des Sciences de la Terre de l'Environnement et de l'Espace of the Université de Montpellier (France) with 20 kV, 10 nA, and 2–5 μm as analytical conditions. A CAMECA SU-30 SEM-probe was also used at the Departamento de Geología, Universidad de Chile (Chile), with 15 kV, 10 nA, and 3–5 μm as analytical conditions.

Results and interpretation of the age data

A summary and detail of the isotopic data are given in Table 1 and Electronic Supplementary Material Table 1 (ESM), respectively. Age and $^{37}Ar_{Ca}/^{39}Ar_K$ ratio spectra are shown in Figs. 2 and 3.

The granodioritic and dioritic plutons

(a) Granodiorite and diorite plutons located 3 km S and SW from the Mantos Blancos deposit

Both samples VO16 and MB02.3 were sampled from the same isolated hill (Fig. 1). Petrographic observations reveal very similar mineralogy, texture, and alteration, and therefore, they could belong to the same magmatic unit, although this could not be unambiguously demonstrated because of the scarcity of rock exposures. Amphiboles from both samples yield discordant plateau ages of 136.8±1.8 Ma and 142.2±1.0 Ma, respectively (Fig. 2). The amphiboles have variable $^{37}Ar_{Ca}/^{39}Ar_K$ ratio spectra indicating that the analyzed amphiboles were slightly altered. It was noted that the apparent ages of sample MB02.3 are affected by much higher error bars than sample VO16 because of the lower measured argon signals. The inverse correlation diagrams ^{36}Ar/^{40}Ar vs ^{39}Ar/^{40}Ar are not shown, but the isochron ages are listed in Table 1. Sample MB02.3 yields an isochron age of 141.8±3.6 Ma, which is concordant with the plateau age, with an initial ^{40}Ar/^{36}Ar ratio of 258.4±22.0 that is slightly lower than the atmospheric ratio. Sample VO16 yields an isochron age of 140.8±2.0 Ma, also concordant with the plateau age, with an atmospheric initial ^{40}Ar/^{36}Ar ratio of 292.6±13.4. If these two samples belong to the same pluton, its age is more probably given by the VO16 plateau age because of the higher precision on the apparent ages and the better fit on the isochron plot. A plateau age of 145.4±0.6 Ma was obtained on the VO16 biotite (Fig. 2). Nevertheless, a slight bump in the shape at intermediate temperatures, typical of slight chloritization and ^{39}Ar recoil during irradiation, clearly appears on the age spectrum. The slightly older plateau age obtained for the biotite compared with the amphibole may be the result of chloritization and/or some excess argon as frequently observed on plutonic biotite. Therefore, the amphibole plateau age for the VO16 sample is preferred. The amphibole sample MB02.4 displays a well-defined plateau age of 141.6±0.6 Ma, corresponding to pure amphibole, as shown by the constant $^{37}Ar_{Ca}/^{39}Ar_K$ ratio spectrum. The two concordant plateau ages of 142.2±1.0 Ma (VO16), and 141.6±0.6 Ma (MB02.4) may indicate that these samples belong to the same plutonic event, in which case, and because of the higher quality of the data displayed by MB02.4, the latter plateau age is preferred for this pluton.

(b) Granodioritic plutons located 8 km SW of the Mantos Blancos deposit

The plateau age of 148.2±0.6 Ma, obtained for the VO8 biotite sample (Fig. 2), suggests the existence of an older

Table 1 Summary of $^{40}Ar/^{39}Ar$ data on biotite, amphibole, plagioclase, and sericitized plagioclase form lava flows, intrusive rocks, and dykes from Mantos Blancos district

Sample	Coordinates		Mineral	Plateau age (Ma, ±2σ)	w.m.a. (Ma, ±2σ)	Steps in plateau or w.m.a.	Percent of Ar released	Isochron age (Ma, ±2σ)	$^{40}Ar/^{36}Ar$ intercept (±2σ)	MSWD	Steps in isochrone age	Integrated age (Ma, ±2σ)	Accepted age (Ma)
	Long W	Lat S											
VO8	70°09′11″	23°28′59″	Bt	148.2±0.6		6–fuse	99.28	148.0±0.8	291.4±40.0	1.2	6–fuse	147.9±0.5	148.2±0.5
VO16	70°05′27″	23°27′06″	Amph	142.2±1.0		7–11	86.60	140.8±2.0	292.6±13.4	1.0	7–11	140.9±1.2	142.2±1.0
VO16	70°05′27″	23°27′06″	Bt	145.4±0.6		4–fuse	95.61	145.5±0.8	247.5±41.7	1.5	4–fuse	144.1±0.5	145.5±0.5
MB02.2	70°05′03″	23°27′23″	Amph	142.5±0.6		10–fuse	79.87	142.4±1.4	261.8±102.6	0.8	10–fuse	141.4±0.3	142.5±0.3
MB02.3	70°05′33″	23°27′17″	Amph	136.8±1.8		11–fuse	81.76	141.8±3.6	258.4±22.0	0.9	11–fuse	136.1±2.1	–
MB02.4	70°04′56″	23°27′28″	Amph	141.6±0.6		5–fuse	98.56	142.3±1.4	269.0±42.1	0.4	5–fuse	141.2±0.5	141.6±0.5
CPM1.27	70°02′53″	23°25′27″	Amph	142.7±2.0		4–fuse	91.54	143.3±5.8	290.1±76.0	1.4	4–fuse	140.3±2.6	142.7±2.0
VO130B	70°03′24″	23°29′59″	Pl	156.3±1.4		4–fuse	84.22	147.8±9.8	442.3±194.6	1.3	4–fuse	155.3±1.4	156.3±1.4
P2.8	70°03′32″	23°25′45″	Pl		142.3±0.7	2–5	35.76	142.3±1.4	296.1±49.5	1.0	2–5	146.3±0.4	142.3±0.7?
					149.3±0.7	8–fuse	46.56	139.9±11.4	763.3±2146.0	1.5	8–fuse	146.3±0.4	149.3±0.7?
S24	70°03′09″	23°25′35″	Pl		139.2±1.0	3–7	54.41	141.5±3.9	239.6±90.7	2.3	3–7	148.3±0.9	?
					162.6±1.9	9–fuse	29.91	151.2±8.0	480.3±133.5	0.1	9–fuse	148.3±0.9	?
VO130B (a)	70°03′24″	23°29′59″	Ser		126.2±0.5	3–5,8	62.11	130.7± 1.9	178.3±50.0	0.7	3–5,8	123.6±0.5	126.2±0.5?
VO130B (b)	70°03′24″	23°29′59″	Ser		147.5±0.7	3–8	63.00	145.2±3.6	357.7±128.2	1.8	3–8	145.8±0.6	147.5±0.5?
VO14 (a)	70°08′38″	23°29′07″	Ser	145.6±0.8		7–fuse	84.15	145.2±1.4	305.3±32.4	0.5	7–fuse	144.6±1.0	145.6±0.8
VO14 (b)	70°08′38″	23°29′07″	Ser	147.1±0.6		2–fuse	92.68	147.1±1.4	295.2±50.0	1.5	2–fuse	146.9±0.5	147.1±0.5
P2.8	70°03′32″	23°25′45″	Ser	101.6±5.0		2–fuse	91.91	107.8±6.7	245.3±66.5	1.1	2–fuse	98.9±5.1	101.6±5.0?
S24 (a)	70°03′09″	23°25′35″	Ser		155.4±0.6	3–6	61.78	154.7±3.6	433.0±1039.4	1.2	3–6	153.2±0.5	155.4±0.6
S24 (b)	70°03′09″	23°25′35″	Ser	154.7±1.2		2–4	80.25	158.3±0.8	6.3±12.1	0.6	2–4	151.4± 1.3	154.7±1.2
DDH11533 104 (a)	70°03′42″	23°25′35″	Ser	155.4±0.7		2–5	70.04	–	No fit	–	–	151.0±0.8	155.4±0.7
DDH11533 104 (b)	70°03′42″	23°25′35″	Ser		156.6±0.5	4–10	59.62	–	No fit	–	–	150.2±0.6	156.6±0.5

The inverse isochrone $(^{40}Ar/^{36}Ar)_i$ ratio and age are calculated from the best-fit line (York 1969). The errors are taken at the 95% confidence limit of York's model-1 fit. The GPS coordinates of the samples are indicated (projection South America 56).

w.m.a. Weighted mean age, $(^{40}Ar/^{36}Ar)_i$ initial ratio from inverse isochrone, *MSWD* mean square of weighted deviates=SUMS/(n−2), *Fuse* total fusion

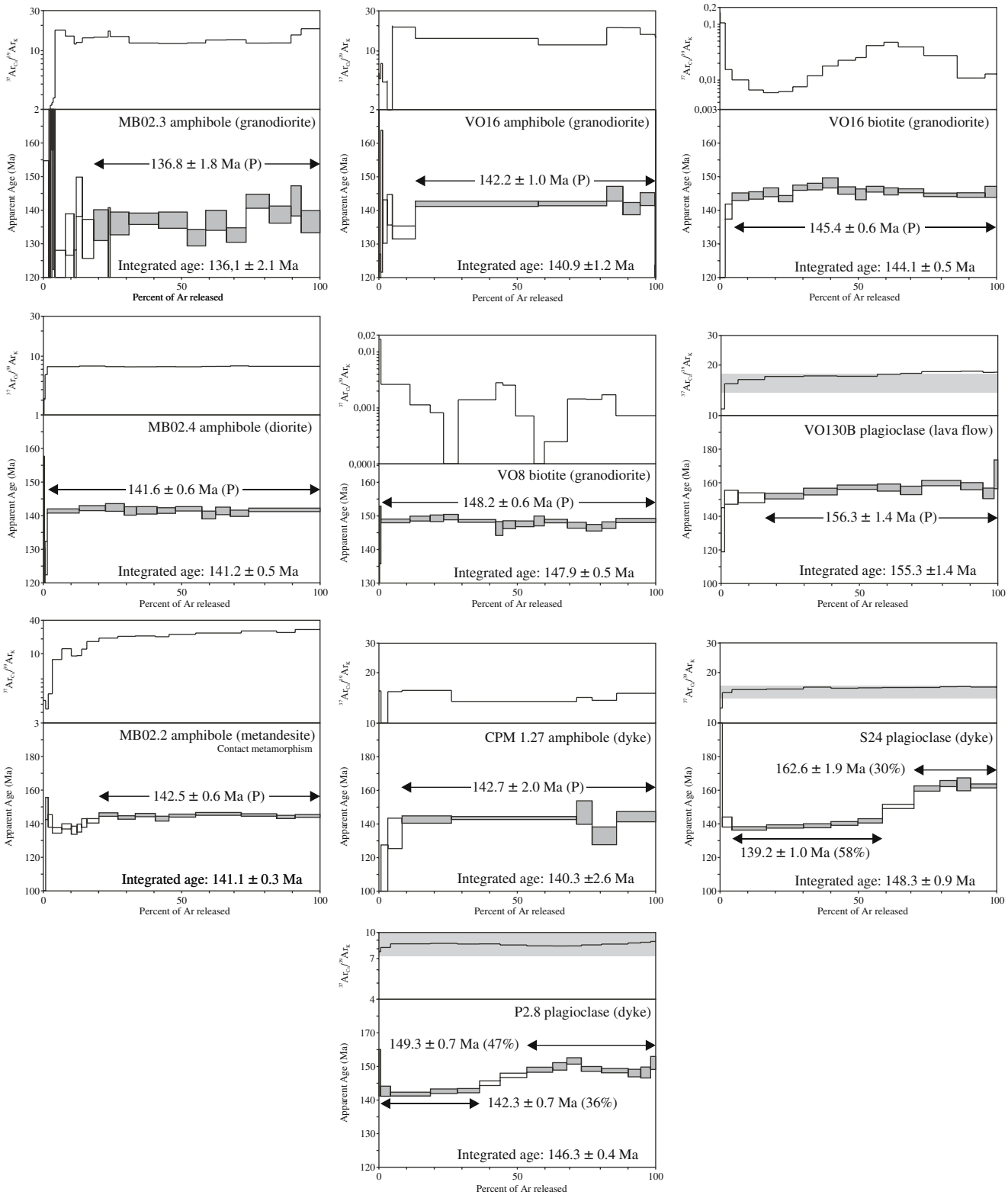

Fig. 2 $^{40}Ar/^{39}Ar$ age and $^{37}Ar_{Ca}/^{39}Ar_K$ ratio spectra obtained on biotite single grain, amphibole, and plagioclase bulk sample and amphibole small grain clusters sample from the Mantos Blancos district (*plutons*, *lava flows*, and *dykes*). *Shaded rectangles* show measured $^{37}Ca/^{39}K$ ratios from microprobe analyses (data on Electronic Supplementary Material Table 2, ESM). Plateau and integrated ages are given at the two sigma (2σ) confidence level; however, apparent ages of each individual step are given at the 1σ (Electronic Supplementary Material Table 1, ESM)

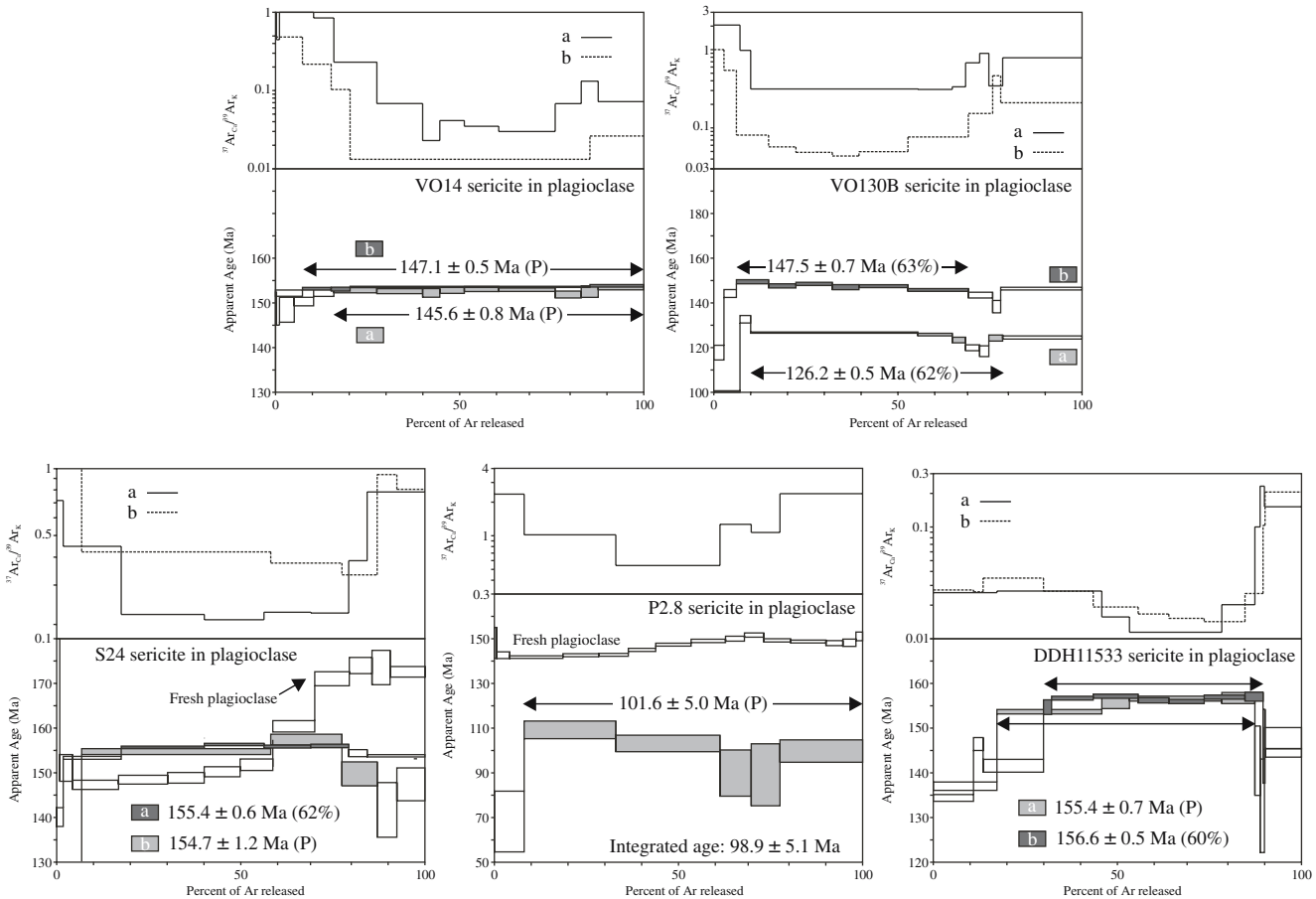

Fig. 3 $^{40}Ar/^{39}Ar$ age and $^{37}Ar_{Ca}/^{39}Ar_K$ ratio spectra obtained on sericitized plagioclases from the Mantos Blancos district. $^{40}Ar/^{39}Ar$ age spectra displayed by fresh plagioclase from samples VO130B, P2.8, and S24 are given for comparison. The criteria to define a plateau age are explained in Fig. 2. Attention

magmatic event. However, some undetected excess argon may affect the biotite from this intrusion.

Volcanic rocks

Plagioclase from a lava flow of the La Negra Formation (sample VO130B) yields a plateau age of 156.3±1.4 Ma on the gas fraction related to the fresh portion of plagioclase, as demonstrated by the nearly flat $^{37}Ar_{Ca}/^{39}Ar_K$ ratio spectrum that is in the range of the Ca/K ratio measured with the electron microprobe (using the relation: $^{37}Ar_{Ca}/^{39}Ar_K$=0.54 Ca/K; Fig. 2). Amphibole from a contact metamorphosed volcanic rock (MB02.2) yielded a well defined plateau age of 142.5±0.6 Ma. The $^{37}Ar_{Ca}/^{39}Ar_K$ spectrum shows a slight increase in this ratio vs temperature, demonstrating that the analyzed mineral was either pure or only slightly altered. This rock is probably included in the contact aureole of the pluton(s) corresponding to samples VO16, MB0.3, and MB02.4. The plateau age is very close to that of the pluton (141.6± 0.6 Ma), and therefore, it is likely that this age represents the intrusive event.

Dykes

Primary amphibole from the late-mineralization dyke (CPM1.27), which crosscuts the hydrothermal breccias of the second mineralization event, yields a plateau age of 142.7±2.0 Ma (Fig. 2) that corresponds to pure amphibole, as shown by the mostly flat $^{37}Ar_{Ca}/^{39}Ar_K$ ratio spectrum. Plagioclase from samples S24 (assumed to be a dyke) and P2.8 (dyke) located inside the main deposit show complex "stair-shaped" age spectra (Fig. 2). These disturbances are not related to K-rich alteration such as sericitation because of the flat $^{37}Ar_{Ca}/^{39}Ar_K$ ratio spectra that are in the range of the Ca/K composition measured on fresh plagioclase by the electron microprobe (Fig. 2). These complex results are discussed further below.

Alteration minerals

Because of their tiny size, secondary minerals such as sericite could not be separated from the plagioclase and therefore were analyzed by heating single grains of strongly altered plagioclase where sericite represents the dominant

alteration mineral. Aguirre et al. (1999) and Fuentes et al. (2005), working with similar material in Cretaceous lavas from the Coastal Cordillera of central Chile, have shown that the obtained plateau ages may represent in some cases the age of the sericite, while the contribution of fresh plagioclase is negligible.

Single grains of strongly altered plagioclase from sample VO14 yield two well-defined plateau ages of 145.6±0.8 Ma and 147.1±0.6 Ma (Fig. 3). The corresponding $^{37}Ar_{Ca}/^{39}Ar_K$ ratios are highly variable and show the dominant degassing of sericite at intermediate temperatures. Both these age values, and the fact that plateau ages are obtained, indicate that the sericite is dominantly degassing on the plateau fraction, and therefore, the plateau ages correspond to the alteration event. Although these ages are not strictly concordant, they are close enough to be considered as representing the same alteration event. Sericitized plagioclase from an andesitic lava flow (sample VO130B) yield widely discordant and much younger apparent ages than the fresh plagioclase of the same rock (156.3±1.4 Ma, Fig. 2). The weighted mean ages are 126.2±0.5 Ma and 147.5±0.7 Ma, considering the 62 and 63% of the total ^{39}Ar released, respectively (Fig. 3). They are obtained when excluding the highest temperature apparent ages because the corresponding high $^{37}Ar_K/^{39}Ar_{Ca}$ ratios suggest that they do not strictly represent sericite degassing. These ages may represent two distinct overprinted alteration events, but this must be confirmed by further work. The oldest age is concordant with the VO14 sericitized plagioclase plateau age.

From within the main orebody, two sericitized plagioclase single grains from sample DDH11533-104 (rhyolitic dome) yielded disturbed age spectra characterized by increasing apparent ages at low temperatures, followed by a flat region, then decreasing ages at high temperatures. These spectra are difficult to interpret because the lowest ages correlate to the highest $^{37}Ar_K/^{39}Ar_{Ca}$ ratios. Nevertheless, one plateau age of 155.4±0.7 Ma is given for one grain, whereas a concordant weighted mean age of 156.6±0.6 Ma was obtained on the other grain (Fig. 3). These two ages correspond to the lowest Ca/K ratios and therefore to the degassing peak of sericite.

The strongly sericitized single grains of plagioclase from the dyke S24 display a similar type of age spectra, with a flat central region yielding a "mini plateau" age of 155.4±0.6 Ma (62% of the ^{39}Ar released) and a plateau age of 154.7±1.2 Ma, both concordant with the DDH11533-104 sericitized plagioclase plateau age (Fig. 3). Curiously, this age is sensibly older than the low intermediate temperature weighted mean age of 139.3±1.0 Ma displayed for the fresh plagioclase of the same sample further discussed later.

The sericitized single grain of plagioclase from the dyke P2.8 displayed apparent ages with large error bars because of the low sericite (K) content of the analyzed grain. An imprecise and young plateau age of 101.6±5.0 Ma was obtained, corresponding to variable $^{37}Ar_{Ca}/^{39}Ar_K$ ratios. Because of the existence of both calcite and albite in this sample and the low quality of the age data, this datum is difficult to interpret.

Discussion

Age of the La Negra Formation

The La Negra Formation, in the Mantos Blancos district, has been precisely dated for the first time; a plateau age of 156.3±1.4 Ma was obtained on plagioclase in an andesitic lava flow (sample VO130B; Fig. 4, Table 2). This age is much younger than previous Rb/Sr age of 186±13 Ma (1σ, MSWD=4.2; Rogers and Hawkesworth 1989) but roughly concordant with the Ar/Ar ages ranging from ca. 150 to 165 Ma, recently reported (Oliveros et al. 2006; Cortés et al. 2007). Judging from all the existing age data, the latest magmatism of the La Negra arc may have occurred in the Mantos Blancos district.

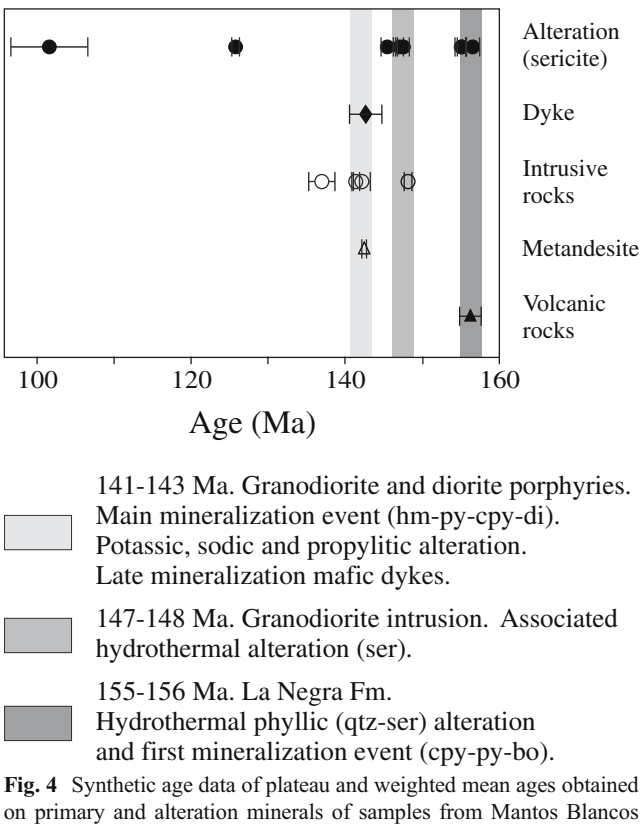

Fig. 4 Synthetic age data of plateau and weighted mean ages obtained on primary and alteration minerals of samples from Mantos Blancos district. *bo*, bornite; *cc*, chalcocite; *cpy*, chalcopyrite; *di*, digenite; *py*, pyrite; *qtz*, quartz; *ser*, sericite. Mineral assemblages are from Ramírez et al. (2006)

Table 2 Rock type, analyzed materials, and geological and chronological interpretation of the accepted $^{40}Ar/^{39}Ar$ ages for the samples from the Mantos Blancos district

Sample	Rock type and analyzed material		Accepted age (Ma)	Age data interpretation
VO130B	Andesitic lava	Pl	156.3±1.4	Age of the volcanism, La Negra Formation, outside from the ore deposit
S24 (a)	Basic dyke	Ser*	155.4±0.6	Age of the phyllic alteration accompanying the emplacement of the rhyolitic dome and the first mineralization event
S24 (b)	Basic dyke	Ser*	154.7±1.2	
DDH11533 104(a)	Rhyolitic dome	Ser*	155.4±0.7	
DDH11533 104(b)	Rhyolitic dome	Ser*	156.6±0.5	
VO8	Granodiorite	Bt	148.2±0.6	Probable age of a plutonic event not related to the Mantos Blancos ore deposit
VO16	Granodiorite	Am	142.2±1.0	Age of plutonic event equivalent to the bimodal stocks and dykes responsible for the main mineralization event inside the Mantos Blancos ore deposit (Ramírez et al. 2006)
MB02.4	Diorite	Am	141.6±0.6	
MB02.2	Metandesite	Am	142.5±0.6	Age of contact metamorphism produced by the intrusion of plutonic rocks represented by VO16, MB02.4, and MB02.3
P2.8	Basic dyke	Pl	142.3±0.7? 149.3±0.7?	Probable ages for the mafic dyke swarm that crosscut the rhyolitic dome inside the Mantos Blancos ore deposit
CPM1.27	Mafic dyke	Am	142.7±2.0	Age of the late stage of the main mineralization event
VO14 (a)	Granodiorite (?)	Ser*	145.6±0.8	Age of different alteration events, most likely not related to the Mantos Blancos mineralization events (samples located far away from the ore deposit)
VO14 (b)	Granodiorite (?)	Ser*	147.1±0.6	
VO130B (b)	Andesitic lava	Ser*	147.5±0.5?	
VO130B (a)	Andesitic lava	Ser*	126.2±0.5?	
P2.8	Basic dyke	Ser*	101.6±5.0?	

Pl Plagioclase, *Ser** sericite in situ in plagioclase, *Am* amphibole, *Bt* biotite

Age of the intrusions

One intrusive magmatic event has been robustly dated in the Mantos Blancos mining district. Dioritic and granodiotitic porphyry intrusions located a few kilometers south from the Mantos Blancos ore deposit (Fig. 1) yield concordant plateau ages of 141.6±0.6 (MB02.4 amphibole) and 142.2±1.0 Ma (VO16 amphibole). These ages are confirmed by sample MB02.2 of a metamorphic rock that belongs to the contact aureole of these plutons, yielding an age of 142.5±0.6 Ma on a metamorphic amphibole (Fig. 4, Table 2). A younger age of 136.8±1.8 Ma obtained on amphibole from sample MB02.3 was rejected because of the lower measured argon signals (see above). A biotite K-Ar age of 147±4 Ma (2σ) previously obtained on a sample from the same outcrop as samples VO16 and MB02.3 (Fig. 1; Chávez 1985) is concordant with our amphibole data. A plateau age of 145.4±0.5 Ma was obtained on biotite from sample VO16, but it displays a bump shaped age spectrum typical of chloritized biotites. The chloritization was confirmed by petrographic observations. Therefore, because biotite from plutonic rocks may be affected by undetectable excess ^{40}Ar and chloritization and without extra age data on other mineral to compare with, it is difficult, at the moment, to evaluate the real meaning of the 4 Ma older $^{40}Ar/^{39}Ar$ age on biotite as well as the K–Ar age from Chávez (1985). As these dated plutons are interpreted to be equivalent to the granodiorite and diorite porphyry stocks and sills of the Mantos Blancos ore deposit, which are supposed to be linked to the second mineralization event inside the copper deposit (Ramírez et al. 2006), an age in the range of 141.6±0.6 Ma and 142.2±1.0 Ma is proposed for this main mineralization event (Fig. 4, Table 2). This age is also consistent with the plateau age of 142.7±2.0 Ma given by the late-mineralization dyke CPM1.27 that crosscuts the hydrothermal breccias of the second mineralization event (Fig. 4, Table 2). This dyke intruded shortly after the intrusion of dioritic and granodioritic porphyries and their associated magmatic-hydrothermal breccias inside the ore deposit.

A granodiorite sample located farther to the SW (VO8, Fig. 1) yielded a plateau age of 148.2±0.6 Ma on biotite, indicating an older magmatic event. Furthermore, a slightly older K–Ar age of 155±4 Ma (Cortés et al. 2007) was obtained on a granodiorite near the VO8 outcrop. Nevertheless, the too-old plateau age obtained on the VO16

biotite compared to amphibole from the same rock leads us to be cautious in the interpretation of the biotite data given by the plutons. Therefore, the various pulses of pluton emplacement based on biotite dating must be verified by analyses of other minerals.

The age spectra displayed by plagioclases of the dykes S24 and P2.8 (Fig. 3) are difficult to interpret. They correspond to flat Ca/K ratios, demonstrating the lack of a K-rich alteration that may have disturbed the isotopic system. The ages obtained on duplicated sericitized plagioclase from sample S24 are higher than the low to intermediate ages of fresh plagioclase (this age is probably valid: see below). Although we cannot dismiss the possibility of excess ^{40}Ar, at least at high temperature, this hypothesis does not explain the younger ages obtained for fresh plagioclase compared to sericite. A possible explanation would be a partial resetting of plagioclase that does not sensibly affect the included secondary sericite. To accept that, we must admit a higher closure temperature for sericite than for plagioclase, and this has never been evidenced to our knowledge. The sericitized plagioclase from sample VO14 that yielded well-defined plateau ages (Fig. 3) consists of a simple mixture system between the two components, plagioclase and sericite (see also examples in Fuentes et al. 2005). These analyzed grains as well as the sericitized plagioclases from samples S24 and P2.8 (Fig. 3) show similar $^{37}Ar_{Ca}/^{39}Ar_K$ ratio spectra. In these diagrams, we clearly observe a first dominant degassing of plagioclase at low temperatures (high $^{37}Ar_{Ca}/^{39}Ar_K$ ratios) followed by a dominant degassing of sericite (low $^{37}Ar_{Ca}/^{39}Ar_K$ ratios) at intermediate temperatures. This means that during the laboratory experiments, the K/Ar system in plagioclase is opened at a temperature where the sericite is still mainly closed. It therefore appears realistic that the low temperature ages (weighted mean= 139.2±1.0 Ma) are the result of a thermal event. This hypothesis is strengthened by the fact that this age is close to the main plutonic and to the second (main) mineralization events. The same conclusions may be deduced for the plagioclase from the dyke P2.8 that displays a low temperature weighted mean age of 142.3± 0.7 Ma that may also be geologically significant. Concerning the fresh plagioclase from samples S24 and P2.8, the high temperature ages of 162.6±1.9 Ma and 149.3±0.7 Ma could represent the emplacement ages for these dykes. A plagioclase age of 151.3±1.2 Ma has been obtained for a coarse pyroxene-plagioclase andesite porphyry dyke within the Manto Blancos main deposit (Cornejo et al. 2006); Maksaev (1990) and Scheuber and González (1999) reported emplacement ages between 139 and 155 Ma for the so-called "nonaltered mafic dykes" in the Coastal Cordillera at the latitude of Mantos Blancos. These K–Ar and Ar–Ar radiometric ages, obtained for plagioclase and whole rocks, are in the same range of our data.

Age of the alteration events

Concerning the strongly sericitized plagioclase data, the $^{40}Ar/^{39}Ar$ age and $^{37}Ar_{Ca}/^{39}Ar_K$ ratio spectra may be complex but are reproducible as demonstrated by the duplicated samples VO14 and DDHH11533.104 (Fig. 3). They are the result of a mixture of mainly plagioclase and sericite but also probably albite and calcite, as observed in thin sections. As previously interpreted by Aguirre et al. (1999) and Fuentes et al. (2005), the apparent ages correlating with the lowest Ca/K ratios are considered as the result of the dominant degassing of sericite. This is strengthened by the existence of corresponding sharp degassing peaks of ^{39}Ar (not shown), characteristic of white micas. These ages, which mostly correspond to intermediate temperature, may be geologically significant.

The strongly sericitized plagioclase sampled in the rhyolitic dome (sample DDH11533.104) yields two concordant ages of 155.4±0.7 Ma (plateau age) and 156.6± 0.6 Ma (mini plateau age). Moreover, the duplicated sericitized plagioclase from sample S24, belonging to a basic rock in the rhyolitic dome, displays a plateau age of 154.7±1.2 Ma and a mini plateau age of 155.4±0.6 Ma that are concordant. These ages represent the first mineralization event. They are close to or concordant with the La Negra primary plagioclase plateau age of 156.3±1.4 Ma (Fig. 4).

Based on mineralogical data (sericite, pyrite, and chalcopyrite inclusions within magmatic quartz phenocrysts) and melt inclusion geochemistry, Ramírez et al. (2006) argued that the phyllic alteration of the first hydrothermal event was probably related to the dome emplacement. However, recent U–Pb ages of 180–181 Ma obtained on zircons form the dome and related volcanic rocks from the Mantos Blancos district have been reported by Cornejo et al. (2006). These age data are sensibly older than our present Ar/Ar ages obtained on sericites related to the first mineralization event. This implies that the emplacement of the dome was not coeval with the first mineralization event, as previously suggested by Ramírez et al. (2006).

The convergence of age data at 155–156 Ma apparently indicates a major geological event, which demarks the origin of (1) La Negra andesitic lava series, (2) the first Mantos Blancos mineralization event, and (3) leucogranitic subvolcanic intrusive rocks located 30 km west of the Mantos Blancos district dated at 155.4±2.5 Ma (Rb–Sr isochrone on nonaltered rocks; Pichowiak 1994). The hydrothermal alteration that accompanied the second mineralization event in the main deposit must have occurred within the same time span proposed for that

mineralization event, which is between 141.6±0.6 Ma and 142.2±1.0 Ma (see above).

The sericitized plagioclase (sample VO14) from an altered pluton located outside the ore deposit (Fig. 1) displays two plateau ages at 145.6±0.8 and 147.1±0.6 Ma. These ages are close to or concordant with a mini plateau age of 147.5±0.7 Ma for a sericitized plagioclase from the andesitic lava flow (sample VO130B). Furthermore, they are similar to the biotite plateau age of 148.2±0.6 Ma calculated for the intrusion of sample VO8 located in the vicinity of the sample VO14 and 10 km to the east of sample VO130B (Fig. 1). If this last age is valid (i.e., no excess argon), the sericite plateau ages may reflect alteration related to the emplacement of plutonic rocks (sample VO8, ca. 148 Ma). It may also represent a regional scale alteration process, as described for volcanic and plutonic rocks in this region (Losert 1974; Sato 1984). Further work is needed to test this hypothesis.

The significantly lower mini plateau age of 125.4±0.4 Ma obtained on sericitized plagioclase from the andesitic lava flow VO130B could represent an overprinted alteration event affecting the volcanic rocks. Sericitized plagioclase from sample P2.8 displays a poor quality result with a poorly constrained plateau age of 101.6±5.0 Ma.

Summary

Nineteen $^{40}Ar/^{39}Ar$ plateau ages were obtained from 11 samples of Jurassic andesitic lava series, intrusive bodies, dykes, and alteration minerals from the Mantos Blancos mining district. Although the data concerning rocks from the ore deposit are complex, the Ar/Ar method seems to be capable of detecting complex histories of successive emplacement, alteration, and thermal resetting on a suite of rock samples.

The La Negra Formation series is precisely dated for the first time on one lava flow from the district at 156.3±1.4 Ma. At least one intrusive magmatic event is precisely dated at 141.6±0.6 Ma (MB02.4) and 142.2±1.0 Ma (VO16). Another older magmatic event at 148.5±0.5 Ma (on biotite) may exist but must be confirmed by extra data.

The first mineralization event and associated phyllic alteration affecting the rhyolitic dome are dated on strongly sericitized plagioclases at around 155–156 Ma and are contemporaneous with the La Negra Formation. These data and recent U/Pb ages on the rhyolitic dome (Cornejo et al. 2006) suggest that the first hydrothermal event is not related to the dome emplacement, as previously suggested by Ramírez et al. (2006). The second and main mineralization event occurred around 142 Ma, as demonstrated by plateau ages obtained on both the intrusions genetically linked to this event and one late-mineralization monzonitic dyke crosscutting the orebody. Hydrothermal events associated with the younger magmatic pulse (~142 Ma), and probably with the older one (~148 Ma), have been detected by analyzing strongly sericitized single grains of plagioclase. A still younger sericitization age at 125.4±0.4 Ma must be confirmed by extra age data.

The geochronological data confirm the existence of two distinct hypogene mineralizing events in the genesis of the Mantos Blancos ore deposit, as proposed by Ramírez et al. (2006).

Acknowledgements This work was financially supported by the Institut de Recherche pour le Développement (IDR), France, and the Consejo Nacional de Ciencia y Tecnología (CONICYT), Universidad de Chile y Angloamerican Mantos Blancos (grant FONDEF project N°1012). M. Manetti is thanked for analytical assistance. S Kojima and an anonymous reviewer are thanked for their helpful comments on the manuscript.

References

Aguirre L, Féraud G, Morata D, Vergara M, Robinson D (1999) Time interval between volcanism and burial metamorphism and rate of basin subsidence in a Cretaceous Andean extensional setting. Tectonophysics 313:433–447

Andriessen PA, Reutter KJ (1994) K–Ar and fission track mineral age determination of igneous rocks related to multiple magmatic arc systems along the 23°S latitude of Chile and NW Argentina. In: Reutter KJ, Scheuber E, Wigger PJ (eds) Tectonics of the Southern Central Andes. Structure and evolution of an active Continental Margin. Springer, Stuttgart, pp 141–153

Arraigada C (2003) Rotaciones tectónicas y deformación del antearco en los Andes Centrales durante el Cenozoico. PhD thesis, Universidad de Chile–Universitè de Rennes 1, France, p 308

Basso M (2004) Carta Baquedano, Región de Antofagasta. Servicio Nacional de Geología y Minería, Carta Geológica de Chile. Serie Geología Básica 82, p 22, 1 map 1:100.000. Santiago

Boric R, Díaz F, Maksaev V (1990) Geología y yacimientos metalíferos de la Región de Antofagasta. Servicio Nacional de Geología y Minería, Chile, Bol 40, p 246

Camus F (2003) Geología de los sistemas porfíricos en los Andes de Chile. Servicio Nacional de Geología y Minería, Chile, p 267

Chávez W (1985) Geological setting and the nature and distribution of disseminated copper mineralization of the Mantos Blancos district, Antofagasta Province, Chile. PhD thesis, University 611 at California, Berkeley, p 142

Cornejo P, Latorre JJ, Matthews S, Marquardt C, Toloza R, Basso M, Rodríguez J, Ulloa C (2006) U/Pb and $^{40}Ar/^{39}Ar$ geochronology of volcanic and intrusive events at the Mantos Blancos copper deposit, II Region, Chile, vol 2. Actas 11th Congr Geológico Chileno, Antofagasta, Chile, pp 129–133

Cortés J, Marquardt C, González G, Wilke H, Marinovic N (2007) Carta Mejillones y Península de Mejillones, Región de Antofagasta. Servicio Nacional de Geología y Minería, Carta Geológica de Chile, Serie Geología Básica, 1 map 1:100.000. Santiago (in press)

Dallmeyer RD, Brown M, Grocott J, Taylor GK, Treolar PJ (1996) Mesozoic magmatic and tectonic events within the Andean plate boundary zone, 26°–27°30′S, North Chile: Constraints from $^{40}Ar/^{39}Ar$ mineral ages. Jour Geol 104:19–40

Espinoza S, Véliz H, Esquivel J, Arias J, Moraga A (1996) The Cupriferous province of the Coastal Range of Northern Chile. In: Camus F, Sillitoe R, Petersen R (eds) Andean Copper deposits: new discoveries, mineralization, styles and metallogeny. Soc Econ Geol Sp Publ 5:19–32

Fuentes F, Féraud G, Aguirre L, Morata D (2005) $^{40}Ar/^{39}Ar$ dating of volcanism and subsequent very low-grade metamorphism in a subsiding basin: example of the Cretaceous lava series from central Chile. Chem Geol 214:157–177

García F (1967) Geología del Norte Grande de Chile, vol 3. Simposium sobre Geosinclinal Andino, Sociedad Geología de Chile, p 138

Grocott J, Brown M, Dallmeyer RD, Taylor GK, Treloar PJ (1994) Mechanism of continental growth in extensional arcs: an example from de Andean plate-boundary zone. Geology 22:391–394

Jourdan F, Vérati C, Féraud G (2006) Intercalibration of the Hb3gr $^{40}Ar/^{39}Ar$ dating standard. Chemi Geol 231:177–189

Kramer W, Siebel W, Romer RL, Haase G, Zimmer M, Ehrlichmann R (2004) Geochemical and isotopic characteristics and evolution of the Jurassic volcanic arc between Arica (18°30′S) and Tocopilla (22°S), North Chilean Coastal Cordillera. Chemie der Erde 65:47–78

Losert J (1974) The formation of stratiform copper deposits in relation to alteration of volcanic series (on north Chilean examples). Rezpravy Č eskolovenské Akad Věd Rocnik 84:1–77

Lucassen F, Franz G (1994) Arc related Jurassic igneous and meta igneous rocks in the Coastal Cordillera of Northern Chile/Region Antofagasta. Lithos 32:273–298

Maksaev V (1990) Metallogeny, geological evolution, and thermo-chronology of the Chilean Andes between latitudes 21° and 26° south, and the origin of major porphyry copper deposits. PhD thesis, Dalhousie University, Canada, p 554

Maksaev V, Zentilli M (2002) Chilean stratabound Cu–(Ag) deposits: an overview. In: Porter TM (ed) Hydrothermal iron oxide copper–gold and related deposits: a global perspective 2. PCG, Adelaide, pp 185–205

Oliveros V, Feraud G, Aguirre L, Fornari M (2006) The early Andean magmatic province (EAMP): $^{40}Ar/^{39}Ar$ dating on Mesozoic volcanic and plutonic rocks from the Coastal Cordillera, Northern Chile. J Volcanol Geoth Re 157:311–330

Oliveros V, Tristá-Aguilera D, Féraud G, Morata D, Aguirre L, Kojima S (2007) Time-relationships between volcanism–plutonism–alteration in Cu-stratabound ore deposits: the Michilla district, northern Chile. A $^{40}Ar/^{39}Ar$ geochronological approach. Miner Deposita (in press)

Palacios C (1978) The Jurassic paleovolcanism in northern Chile. PhD thesis, Tubingen University, Germany, p 99

Palacios C (1984) Considerations about the plate tectonic models, volcanism, and continental crust in the southern part of the Central Andes. Tectonophysics 108:205–214

Palacios C (1990) Geology of the Buena Esperanza copper–silver deposit, Northern Chile. In: Fontboté L, Amstutz GC, Carozo M, Cedillo E, Frutos J (eds) Stratabound ore deposits in the Andes. Springer, Berlin Heidelberg New York, pp 313–318

Pichowiak S (1994) Early Jurassic to Early Cretaceous magmatism in the Coastal Cordillera and the Central Depression of North Chile. In: Reutter KJ, Scheuber E, Wigger PJ (eds) Tectonics of the Southern Central Andes. Structure and evolution of a continental margin. Springer, Stuttgart, pp 203–217

Pichowiak S, Buchelt M, Damm KW (1990) Magmatic activity and tectonic setting of early stages of Andean cycle in northern Chile. Geol Soc Am Sp Paper 241:127–144

Ramírez L, Palacios C, Townley B, Parada M, Sial AN, Fernandez-Turiel JL, Gimeno D, García-Valles M, Lehmann B (2006) The Mantos Blancos copper deposit: an upper Jurassic breccia-style hydrothermal system in the Coastal Range of northern Chile. Miner Deposita 41:246–258

Renne PR, Swisher CC, Deino AL, Karner, DB, Owens T, De Paolo DJ (1998) Intercalibration of standards, absolute ages and uncertainties in $^{40}Ar/^{39}Ar$ dating. Chem Geol Isotope Geoscience Section 145:117–152

Rogers G, Hawkesworth CJ (1989) A geochemical traverse across the North Chilean Andes: evidence for crust generation from the mantle wedge. Earth Planet Sci Lett 91:271–285

Sato T (1984) Manto type copper deposits in Chile, a review. Bull Geol Survey Jpn 35:565–582

Scheuber E (1994) Tektonische Entwicklung des nordchilenischen aktiven Kontinentalrandes: Der Einfluss von Plattenkonvergenz und Rheologie. Geotekton Forsch 81:1–131

Scheuber E, González G (1999) Tectonics of the Jurassic-Early Cretaceous magmatic arc of the north Chilean Coastal Cordillera (22°–26°S): a story of crustal deformation along a convergent plate boundary. Tectonics 18:895–910

Steiger RH, Jäger E (1977) Subcommission on geochronology: convention on the use of decay constants in geo- and cosmology. Earth Planet Sci Lett 36:359–362

Tassinari C, Munizaga F, Ramírez R (1993) Edad y geoquímica isotópica Rb-Sr del yacimiento de cobre Mantos Blancos: relación temporal con el magmatismo jurásico. Rev Geol Chile 20:193–205

Tristá-Aguilera D, Barra F, Ruiz J, Morata D, Talavera-Mendoza O, Kojima S, Ferraris F (2006) Re–Os isotope systematics for the Lince–Estefanía deposit: constraints on the timing and source of copper mineralization in a stratabound copper deposit, Coastal Cordillera of Northern Chile. Miner Deposita 41: 99–105

Turner G, Huneke JC, Podose FA, Wasserbrug GJ (1971) $^{40}Ar/^{39}Ar$ ages and cosmic ray exposure ages of Apollo 14 samples. Earth Planet Sci Lett 12:15–19

York D (1969) Least squares fitting of a straight line with correlated errors. Earth Planet Sci Lett 5:320–324